ANALYSIS OF TOPOGRAPHIC ROUGHNESS OF MARTIAN AND HAWAIIAN TERRAINS. A. R. Morris[1], F. S. Anderson[1], P. J. Mouginis-Mark[1], A. F. C. Haldemann[2], and H. Garbeil[1], [1]Hawai'i Institute for Geophysics and Planetology, 1680 East-West Rd, POST 504, Honolulu, HI 96822 (aisham@hawaii.edu), [2]JPL, Caltech, Pasadena, CA, 91109.

Introduction: Using the method of calculating fractal statistics described in detail by [1], we develop two-dimensional maps of the Hurst exponent of Martian analog flows in Hawaii to understand the effects of limited resolution topographic and imaging data on the interpretation of volcanic features on the surface of Mars. We seek to understand the effects of dataset resolution for TOPSAR, lidar, and photoclinometry data on the interpretation of various volcanic surfaces on Kilauea volcano, with applications to rover traverse navigation on planetary surfaces.

Background: The roughness of a natural surface is often defined by the topography of the surface at scales of a few tens of meters or less and can be quantitatively described by self-affine, or fractal, statistics [e.g. 1-3]. To ensure the safety of rovers and scientific instruments on Mars, these scales are of critical importance during landing site selection and rover traverse operations [4]. Published work on terrestrial [1-3] and Martian topography datasets [5-7] has demonstrated that statistical values such as the Hurst exponent can be used in conjunction with other statistical measures such as RMS slope to understand the relationship between scale-dependent roughness characteristics and the morphology of a surface.

Data: Extensive Light Detection and Ranging (lidar) coverage of the summit of Kilauea volcano on the Big Island of Hawaii (30 cm posting, 1 m DEM with ~2 cm vertical resolution [8]) provides an opportunity for simulating higher resolution Martian topography data such as will be obtained from photoclinometry and stereo imaging using the High Resolution Imaging Science Experiment (HiRISE) and Context Imager (CTX) cameras on Mars Reconnaissance Orbiter (MRO). Topographic Synthetic Aperture Radar (TOPSAR) data is also available over the summit of Kilauea. The TOPSAR DEM has a 10 m spatial resolution and 2 m vertical accuracy [9].

In addition to the lidar and TOPSAR data, we use high resolution topography generated from controlled stereo imaging of volcanic surfaces within Kilauea caldera to provide a detailed view of sub-meter surface roughness of the young volcanic terrains covered by the lidar data. To obtain the stereo data, we moved a 12.8 megapixel digital camera, pointed perpendicular to the ground, along a horizontal bar mounted between two leveled tripods (Fig. 1). We were able to collect extremely high-resolution (~1 mm pixel) stereo images of various surfaces that were subsequently transformed into controlled DEMs.

We use the DEMs from these three datasets to examine the surface roughness of six sites within the caldera of Kilauea volcano by calculating statistical values to quantify surface roughness characteristics.

Figure 1. Example field set-up. 12.8 megapixel camera is suspended between two tripods. Images are taken every 10 cm and stereo matching is performed back in the lab.

Methods: Following [1], we define surface roughness as the topographic expression of the surface at horizontal scales from sub-meter to hundreds of meters. Previous workers, despite noting that the roughness of natural surfaces often exhibits anisotropic behavior [1], were typically confined to analyses in one dimension [e.g. 1-3]. In order to address possible anisotropic behavior, as well as greatly enlarge the available roughness dataset for a given investigation, we have expanded the profile approach to a two-dimensional approach, ideal for use with regularly posted DEMs.

The DEM is first divided into groups of pixels, termed cells, of a size selected to accurately obtain statistically valid results. Next, all possible offsets (steps) between pixels are identified. The RMS deviation of a point on the surface as a function of step size is then calculated for all pixel pairs within the cell and is given by

$$\upsilon(\Delta x,\Delta y)=\sqrt{\frac{1}{m}\frac{1}{n}\sum_{i=i}^{m}\sum_{i=1}^{n}\left[z(x_i,y_i)-z(x_i+\Delta x,y_i+\Delta y)\right]^2} \qquad (1)$$

where m and n are the number of samples in the x and y directions, z is the elevation, and Δx and Δy equal the step size in the x and y directions. The deviation needs to be calculated for all step sizes of the same magnitude, though this may represent different lateral and vertical shifts of the DEM , so we determine the scalar distance of a shift by $\Delta d = \sqrt{\Delta x^2 + \Delta y^2}$. The RMS deviation of self-affine surfaces is a power law that scales between scalar distance (Δd) and ν(x,y):

$$\upsilon(x,y) = \upsilon(\Delta d_0)\left[\Delta d / \Delta d_0\right]^H = \upsilon_0\left[\Delta d / \Delta d_0\right]^H \quad (2)$$

where H is the Hurst exponent (0> H >1), a constant over a given range of horizontal scales. The RMS deviation and step size are plotted against one another and the resulting graph is called a deviogram (Fig. 2). The slope of the line on the deviogram is the Hurst exponent, where changes in the Hurst exponent indicate changes in the process affecting the surface roughness at that scale [1]. We use the calculated RMS deviation and the step size to derive a deviogram and an average Hurst exponent for each cell. The cells are then mapped as an image, providing a quantitative 2-D view of surface roughness.

Results and Discussion: We have included the deviogram for one Kilauea site as an example of the results of our analysis (Fig. 2). This field site is located within a devitrified, oxidized compound pahoehoe flow field. At the scale of the stereo-derived DEM, the deviogram in Fig. 2 appears to steepen at approximately 1-2 cm, likely indicative of the effective surface roughening as a result of the spalling off of the glassy selvage from the surface of the flow. To complement the stereo data, we anticipate using a tripod-mounted lidar system to obtain additional sub-centimeter topography of the surfaces within Kilauea caldera.

Analysis of deviograms from the six selected sites within the caldera indicates variations in Hurst exponent do occur within the deviograms calculated for each of the individual field sites. Particularly at the stereo and lidar scales, we begin to observe differences in deviogram and Hurst exponent among surfaces that exhibit variations in surface character. We continue to investigate the nature of these variations and it appears we will be able to quantify surface types based upon deviogram characteristics and Hurst exponent values.

In addition to the terrestrial ground-truth of this technique, we have also applied the model to the global 1/128º MOLA DEM. The initial results are promising (Fig. 3), as we observe similar roughness characteristics as described by [5-7]. The high surface roughness in areas such as Valles Marineris and the southern highlands and the very low roughness of the north polar erg are apparent at the 300 m to 3 km scales, which are limited by the MOLA resolution. We continue to analyze the MOLA-based roughness data, in addition to eagerly awaiting the HiRISE and CTX stereo data for high resolution roughness investigations of lava flow types and degradation states in order to infer spatial variations in eruption style and magnitude, following our work on lava flows in Hawaii.

References: [1] Shepard et al. (2001) *JGR, 106,* 32,777-32,795. [2] Shepard et al. (1995) *JGR, 100,* 11,709-11,718. [3] Campbell et al. (2003) *GRL, 30,* doi:10.1029/2002GL016550. [4] Anderson et al. (2003) *JGR, 108,* doi:10.1029/2003JE002125. [5] Kreslavsky and Head (2000), *JGR, 105,* 26,695-26,711. [6] Aharonson et al. (2001), *JGR, 106,* 23,723-23,735. [7] Orosei et al. (2003), *JGR, 108,* doi:10.1029/2002JE001883. [8] Mouginis-Mark and Garbeil (2005) *Rem. Sens. Eniv., 96,* 149-164. [9] Rowland et al. (1999), *Bull. Volc., 61,* 1-14.

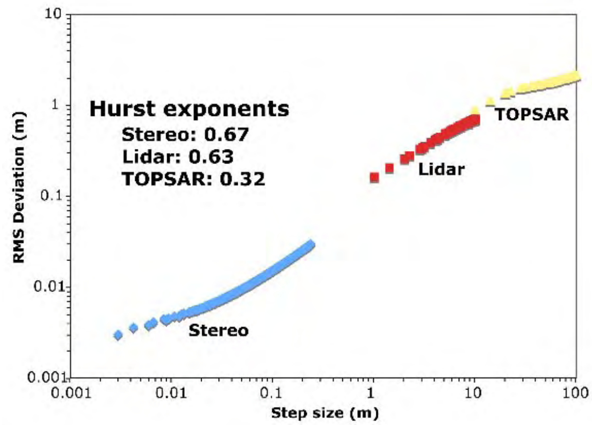

Figure 2. Example deviogram from selected field site. RMS deviation from each dataset is color coded. Note consistency in trend from stereo to lidar and first few step sizes at TOPSAR scale.

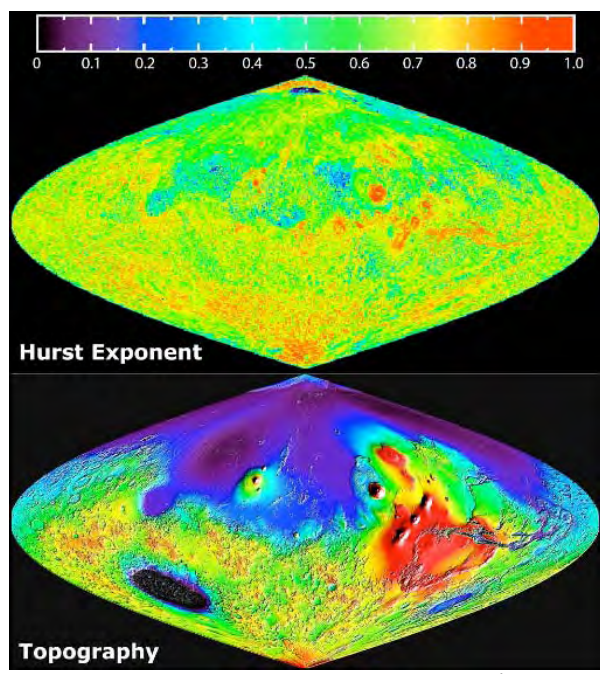

Figure 3.a. Global Hurst exponent map of Mars derived using 30 km cells. **3.b**. MOLA topography draped over shaded relief.